Pergamon

Int. J. Solids Structures Vol. 33, No. 13, pp. 1891–1901, 1996

0020-7683/96 $15.00 + .00

0020-7683(95)00137-9

INTERIOR ENERGY FOCUSING WITHIN AN ELASTO-PLASTIC MATERIAL

M. TADI, HERSCHEL RABITZ
Department of Chemistry, Princeton University, Princeton, New Jersey 08544, U.S.A.

YOUNG SIK KIM
Department of Applied Science, Hong-IK University, Mapoku, Seoul 121, Korea

ATTILA ASKAR
School of Sciences, Koc University, Bebek-Istanbul, Turkey

JEAN H. PREVOST
Department of Civil Engineering and Operations Research, Princeton, New Jersey 08544, U.S.A.

and

JOHN B. McMANUS
Aerodyne Research Inc., Billerica, Massachusetts 01821-3976, U.S.A.

(*Received* 13 *December* 1994; *in revised form* 3 *June* 1995)

Abstract—In this paper we consider the problem of focusing acoustic energy within a subsurface volume in a solid by means of a designed surface pattern, and ask how that focusing is affected by plastic yield of the material. Surface force patterns that yield efficient subsurface acoustic focusing have been designed using optimal control theory, based on a linear elastic model of a solid. The acoustic waves generated by these forces then are propagated, via numerical algorithms, in a model solid that exhibits plastic yield. Numerical results indicate that as the amplitude of the force increases, yield begins to develop at the focus, with the formation of an expanding region of permanent plastic deformation. Despite the occurrence of yield near the focus, acoustic energy still can be delivered to the focal volume with good efficiency.

1. INTRODUCTION

Optimal control theory (OCT) recently has been applied to the design of patterns of surface forces that produce efficient subsurface acoustic focusing in solids (see e.g. Kim *et al.*, 1991; 1995). We previously have used OCT to design either normal, Kim *et al.* (1991), or tangential force patterns, Kim *et al.* (1995), for acoustic focusing, while simultaneously minimizing the total expended energy and the disturbance of the solid away from the focus. Since there are some applications where a high amplitude acoustic pulse may be useful, we consider here the effect of material yield on the propagation of acoustic waves generated by these force patterns. A simple viscoplastic model of a solid is used in a numerical algorithm to propagate waves from a pattern of normal forces that gives optimal focusing in a linear elastic solid. We calculate the acoustic energy delivered to the target volume as the strength of the applied force is increased beyond the onset of plastic yield.

There are a number of applications of focused acoustic waves in solids, and new opportunities may be opened by an ability to conveniently produce a high intensity focus. Acoustic nondestructive testing often makes use of focused waves for localized subsurface inspection (see e.g. Cielo *et al.*, 1985). A high intensity focus may be used to probe nonlinear elastic properties to, for example, evaluate bond properties (Lemons and Kompfner, 1985). We have suggested potential applications based on very high acoustic amplitudes that might be delivered by a laboratory scale apparatus. Large scale devices and experiments that generate very high acoustic amplitudes have been used for bonding (Robinson, 1977),

inducing chemical or phase changes (Duval and Graham, 1977), and removal of material at blind surfaces (Boustic and Cottet, 1991). We have shown that efficient subsurface acoustic focusing, with minimal disturbance away from the focus, should be achievable by careful design of a pattern of forces acting on the surface. Such forces might be produced by laser-surface interactions.

Acoustic wave generation via laser-surface interactions has been demonstrated over a wide range of intensities (Scruby *et al.*, 1980). At low laser intensities, the material surface is simply heated and acoustic waves are generated by the tangential forces arising from thermal expansion. At higher laser intensities, the surface can be ablated and stronger acoustic waves are produced by the normal forces arising from material recoil. Using very high power lasers, ablation of target surfaces can produce shock waves and significant compression. We do not address such extreme intensities in the work described here. Rather, we consider pressure regimes that may be produced by more modest laser powers, ablating a sacrificial film coating instead of the bulk material (Tam and Do, 1992).

Designing surface forces to produce an efficient focus is a complicated problem because forces acting on solid surfaces produce a mixture of bulk shear and compressional waves with strong angular dependence, as well as surface (Rayleigh) waves (see e.g. Fortov *et al.*, 1991). The complexity is increased if other constraints are included, such as a desire not to disturb the solid away from the focus, or to limit the total energy expended. Optimal control theory provides a systematic means of generating such designs, since it naturally includes the response of the system, the goal to be achieved, and penalties to be avoided. We previously have used OCT to design both normal (see e.g. Kim *et al.*, 1991) and tangential force patterns (see e.g. Kim *et al.*, 1994) for acoustic focusing, while simultaneously minimizing the total expended energy and the disturbance of the solid away from the focus. Higher pressures can be achieved with normal forces, so in this paper that is the only type of force we consider (corresponding approximately to laser ablation). With the goal of maximizing the total acoustic energy within a defined volume, the resulting surface force patterns have the form of a pair of concentric rings that converge radially. As much as 23% of the input mechanical energy can be localized in the target volume at a specified time.

In the work presented here, we investigate the effects that occur as the amplitude of the focused acoustic field from a designed laser pulse begins to reach a regime where material nonlinearity and yield occurs. To incorporate the nonlinear behavior of the material directly in the optimal control formulation would require very large computational resources. However, this should not be necessary at the onset of yield because the waves will be transmitted linearly through the material until they converge and reach high amplitude near the target volume. Therefore, here we will examine the effects of using force patterns that are based upon a linear elastic solid, and propagating the resultant acoustic waves through a solid where yield can occur. An additional goal of this work is to see how hard one needs to push on the surface in order for subsurface yield to occur.

In Section 2 we briefly review the optimal control problem detailed in earlier work by Kim *et al.* (1991) to obtain the optimal surface loads. Section 3 summarizes the elasto-visco-plastic model employed for the material and Section 4 is devoted to numerical results.

2. THE OPTIMAL ACOUSTIC CONTROL PROBLEM

In this section we briefly summarize the optimal acoustic control problem. In this paper we do not formulate the optimal control problem for elasto-plastic solids. Rather, we study the effectiveness of an optimal load designed for a linear elastic material applied to a material that has plasticity effects present.

Optimal control theory is used to compute the optimal normal surface loading that is aimed at focusing a certain amount of acoustic energy E_p (strain plus kinetic) in a target volume within the solid. The energy focusing in the target volume is to occur at a particular time in an efficient manner such that the total disturbance elsewhere in the material remains

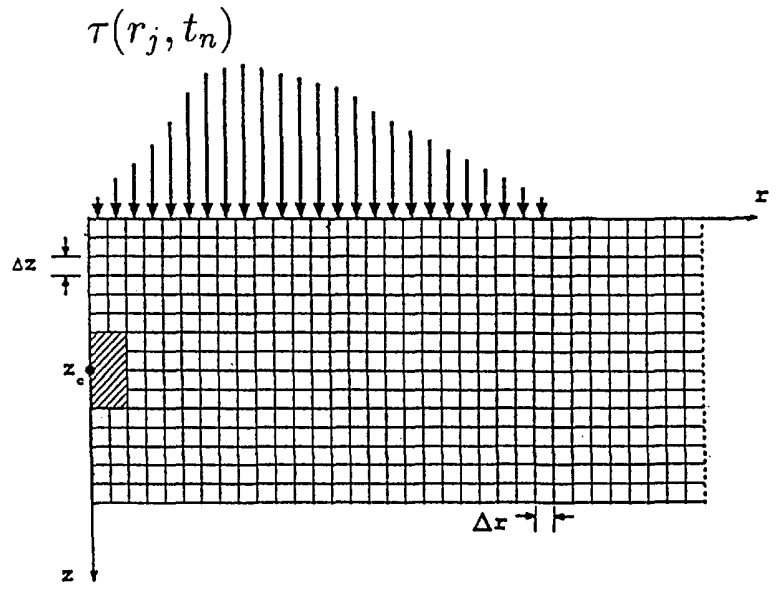

Fig. 1. A cut through the axi-symmetric half space under surface load $\tau(r_j, t_n)$ schematically indicated by the vertical arrows. The axis of symmetry is z and the shaded area is the target volume. The target volume is centered at z_c which is located 0.32 cm from the surface.

as small as possible. The geometry of the isotropic, homogeneous elastic half space is shown in Fig. 1.

There are several essential elements in any optimal control problem. One derives a functional that represents the end state of the system (e.g. focused acoustic waves), costs to be avoided (e.g. disturbance away from the focus), and the underlying physical behavior of the system (acoustic wave equation). Minimizing the functional results in the designed system inputs (space-time force patterns) that best satisfy the goals with minimum costs. Here, the objective functional to be minimized is written as:

$$J(u_i, \tau_i) = \Phi(T) + L_1 + L_2, \tag{1}$$

where u_i and τ_i are displacements and surface tractions, and $\Phi(T)$ is given as

$$\Phi(T) = \left| \int_{V_c} \varepsilon(x, T)\, \mathrm{d}V - E_P \right|. \tag{2}$$

Here, the energy density $\varepsilon(x, t)$ is given as

$$\varepsilon(x, t) = \tfrac{1}{2}\rho \dot{u}_i \dot{u}_i + \int_0^t \sigma_{ij} \dot{\varepsilon}_{ij}\, \mathrm{d}t, \tag{3}$$

where ε_{ij} and σ_{ij} are strain and stress tensors (which are related through Hook's law), and repeated indices correspond to summation over all components. The first term is the kinetic energy density and the second term is the strain energy density. In eqn (2) the parameter $\Phi(T)$ is the difference between the energy in the target volume V_c at the target time T and a desired value E_P. The cost functionals L_1, L_2 are given as

$$L_1 = w_1\left[\int_V \int_0^T \varepsilon(x,t)\,\mathrm{d}t\,\mathrm{d}V - w_1' \int_{V_c} \varepsilon(x,T)\,\mathrm{d}V\right] \tag{4}$$

$$L_2 = \frac{w_2}{2}\int_S \int_0^T \tau_i^2\,\mathrm{d}t\,\mathrm{d}s. \tag{5}$$

The functional L_1 represents the disturbance to the system except in the target volume, and L_2 is a measure of the total surface force during the process. The weight factors (w_1, w_1', w_2) represent the relative importance of the penalty terms in the objective functional, and introduce flexibility in the design process. For example, a nonzero value for w_1 corresponds to focusing energy at the target with the introduction of minimum disturbances elsewhere in the solid, while a nonzero value for w_2 corresponds to achieving the objective with the application of minimum surface loads. For a linear elastic isotropic material the equation of motion is given by

$$\mu\frac{\partial^2 u_i}{\partial x_j \partial x_j} + (\lambda+\mu)\frac{\partial^2 u_j}{\partial x_j \partial x_i} = \rho\ddot{u}_i, \quad (x,t)\in V\times T^+, \tag{6}$$

and initial conditions are given as

$$u_i(x,0) = \dot{u}_i(x,0) = 0, \quad x\in V. \tag{7}$$

The applied surface tractions act on the system through the boundary conditions

$$\mu\frac{\partial u_i}{\partial x_j}n_j + \mu\left(\frac{\partial u_j}{\partial x_j} + \frac{\partial u_j}{\partial x_i}\right)n_j = \tau_i, \quad (x,t)\in S\times T^+, \tag{8}$$

where n_j is the direction cosine of the unit vector normal to the surface, and λ and μ are Lame's constants.

The problem now is to minimize the cost functional $J(u_i, \tau_i)$ given by eqn (1) subject to constraints of the equations of motion given by eqns (6–8). Lagrange multipliers ψ_i are introduced to formulate this problem as an unconstrained optimization problem. The modified cost functional is then given by

$$\bar{J}(u_i,\tau_i,\psi_i) = J - \int_V \int_0^T \psi_i\left[\mu\frac{\partial^2 u_i}{\partial x_j \partial x_j} + (\lambda+\mu)\frac{\partial^2 u_j}{\partial x_j \partial x_i} - \rho\ddot{u}_i\right]\mathrm{d}t\,\mathrm{d}V. \tag{9}$$

The necessary condition for $\bar{J}$ to be stationary is that

$$\delta\bar{J}(u_i,\tau_i,\psi_i) = 0. \tag{10}$$

Optimality conditions are derived from the fact that the variations δu_i, $\delta\tau_i$ and $\delta\psi_i$ are independent, and therefore their coefficients must vanish, independently. The Lagrange multipliers are required to satisfy a set of equations corresponding to $\delta\bar{J}/\delta u_i = 0$. The demand $\delta\bar{J}/\delta\tau_i = 0$ specifies the optimal loads.

For numerical implementation, the optimal loads are solved iteratively using a mathematical programming technique with discretized space and time. The procedure is to assume an initial value for the surface tractions τ_i and then integrate the equations of motion forward and compute the value of the cost functional. An update to the τ_i's is obtained using the conjugate gradient method. This procedure is repeated until $\delta\bar{J}\delta\tau_i$ is zero within a specified tolerance.

The above procedure places no constraint on the sign of the surface load, and in practice it is not always possible to produce negative surface loads. To avoid negative loads, the surface tractions can be defined by

$$\tau_i(r, t) = -\tfrac{1}{2}p_i^2(r, t). \tag{11}$$

Accordingly, the surface load's can only have positive values. A modified cost functional L_2 is then defined by

$$L_2 = \frac{w_2}{2}\int_S \int_0^T p_i^2 \, \mathrm{d}t \, \mathrm{d}S. \tag{12}$$

Figure 2 shows an optimal loading calculated using the above algorithm. The surface loads are constrained to be positive and the weight factors are chosen as $w_1 = 0.32$, $w_2 = 0$, $w_1' = 0.03$. Thus, this pattern is designed to minimize disturbance away from the focus but does not impose a penalty on the peak force used. The loading has the form of a pair of radially symmetric rings that converge toward the center. The symmetry of the loading allows the plot to be shown as a function of normalized radius and time.

In the work by Kim *et al.* (1991), optimal surface loads were computed for four different sets of weight factors, corresponding to different choices of costs. The results of the calculations with different sets of weights were qualitatively the same. All sets of weights resulted in converging ring loads, but with varying focusing efficiencies. In the work that follows, we will use only one of the computed optimal load patterns as shown in Fig. 2.

3. ELASTO-VISCO-PLASTIC MATERIAL

Next, we state the particular model that is used to study the plasticity effects on the interior focusing of acoustic energy. This model is presented in detail by Loret and Prevost (1990) and is a good first order approximation for most metals. A similar model is used by Fortov *et al.* (1990) for studing spallation of metals under laser irradiation. In the following, the generalized elasto-visco-plastic stress-strain relationship as proposed by Duvaut and Lions (1972) is used:

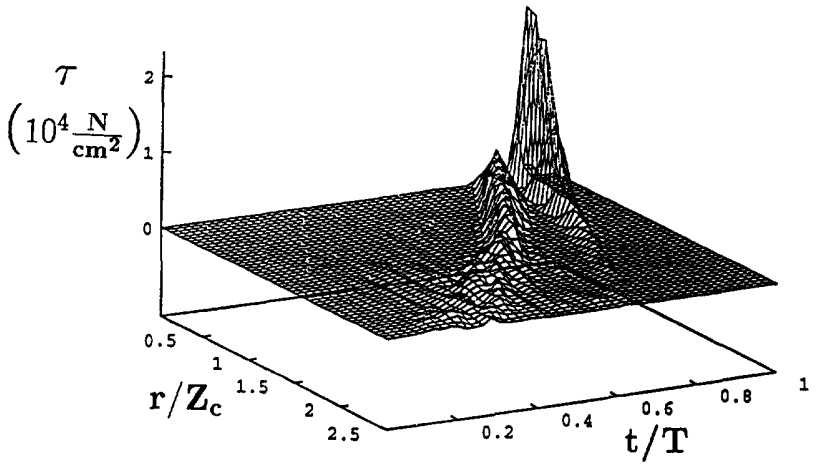

Fig. 2. Computed pattern of optimal surface loading to produce a subsurface acoustic focus. The circularly symmetric pattern is plotted as a function of normalized radius (r/Z_c) and (t/T), in units of 10^4 N/cm^2.

$$\dot{\sigma}_{ij} = 2\mu\dot{\varepsilon}_{ij} + \lambda\dot{\varepsilon}_{kk}\delta_{ij} - \frac{1}{\eta}(\sigma_{ij} - \bar{\sigma}_{ij})\mathscr{H}(f(\sigma_{ij})), \tag{13}$$

where $\bar{\sigma}_{ij}$ is the projection of the stress σ_{ij} on the yield surface, η is the relaxation time and $\mathscr{H}$ is the Heaviside function. For $\eta = 0$ instantaneous relaxation takes place ($\bar{\sigma}_{ij} = \sigma_{ij}$) and the model reduces to that of an inviscid elasto-plastic material, where as for $\eta > 0$, the response is delayed. In the limit of $\eta \to \infty$ the model reduces to the linear elastic case. The relaxation time η induces a length scale $c_d\eta$ and is related to the microstructure of the material where c_d is the speed of the compressional wave. Here, η is used as a parameter to make the transition across the plasticity surface smooth. In the following, the actual choice for η is dictated by numerical considerations discussed below. The material is assumed to exhibit Von-Mises elasto-plastic behavior for which the form of the yield function $f(\sigma_{ij})$ is given by:

$$f(\sigma_{ij}) = (J_2)^{1/2} - c, \tag{14}$$

where J_2 is given in terms of the stress deviator tensor by:

$$J_2 = \tfrac{1}{2}s_{ij}s_{ij}, \quad s_{ij} = \sigma_{ij} - \tfrac{1}{3}\sigma_{kk}\delta_{ij}. \tag{15}$$

The parameter c is the yield stress of the material in pure shear.

4. NUMERICAL RESULTS AND DISCUSSIONS

In this section we present numerical results for the problem of focusing acoustic energy within an elasto-plastic medium. The finite element scheme that is used is given by Prevost and Loret (1990) for a planar problem. Here we apply the scheme to the present axi-symmetric geometry. The calculations are based on the physical properties of an aluminum alloy given in Kim *et al.* (1991), where the mass density is $\rho = 2.77\,\text{g/cm}^3$, and Lame's constants are $\lambda = 0.546 \times 10^{12}\,\text{g/cmsec}^2$ and $\mu = 0.257 \times 10^{12}\,\text{g/cmsec}^2$. For the yield stress in pure shear we use $0.19 \times 10^{10}\,\text{dyne/cm}^2$. The computational domain is shown in Fig. 1 which is similar to the axisymmetric geometry used in Kim *et al.* (1991). The computational domain is extended in both directions so that reflections from the boundaries have negligible effect on the target energy. Since the computational domain has been extended, and the number of mesh points is limited, the target volume is made relatively large so that it contains enough mesh points. The target volume is a cylinder that extends from $z = 0.24$ to 0.4 cm below the surface, and has a radius of 0.08 cm. We assume zero boundary conditions for the right and lower sides

$$u_r(t, z, 2) = u_z(t, z, 2) = u_r(t, 0.8, r) = u_z(t, 0.8, r) = 0, \tag{16}$$

and for the left side i.e., the symmetry axis, we have the symmetric boundary conditions, $u_r(t, z, 0) = 0$, where $u_r(t, z, r)$ and $u_z(t, z, r)$ are the displacements in the r and z directions respectively. The applied surface loads are distributed over the upper boundary and are given as a function of time. The target time (T) is chosen to be 4.5 μs, which is long enough for the longitudinal and shear waves to interact and reach the target. Numerical experiments with larger domains showed that the reflections from the boundaries using the above computational domain have little effect on the target energy. The finite element mesh is generated by dividing the z and r directions into equal intervals. Explicit time integration is used which requires the time step size to be less than (l_{mm}/c_d) for stability, where c_d is the longitudinal wave velocity and l_{mm} is the shortest length in the elements. To assure that the results do not exhibit any mesh dependency we started with a $(r \times z) = (50 \times 20)$ mesh and then compared the results to the cases where we used (50×30) and (50×40) meshes. The results were the same and the value of the energy at the target also converged. For all the computations the conservative (50×40) mesh is used. We apply the optimal loading shown

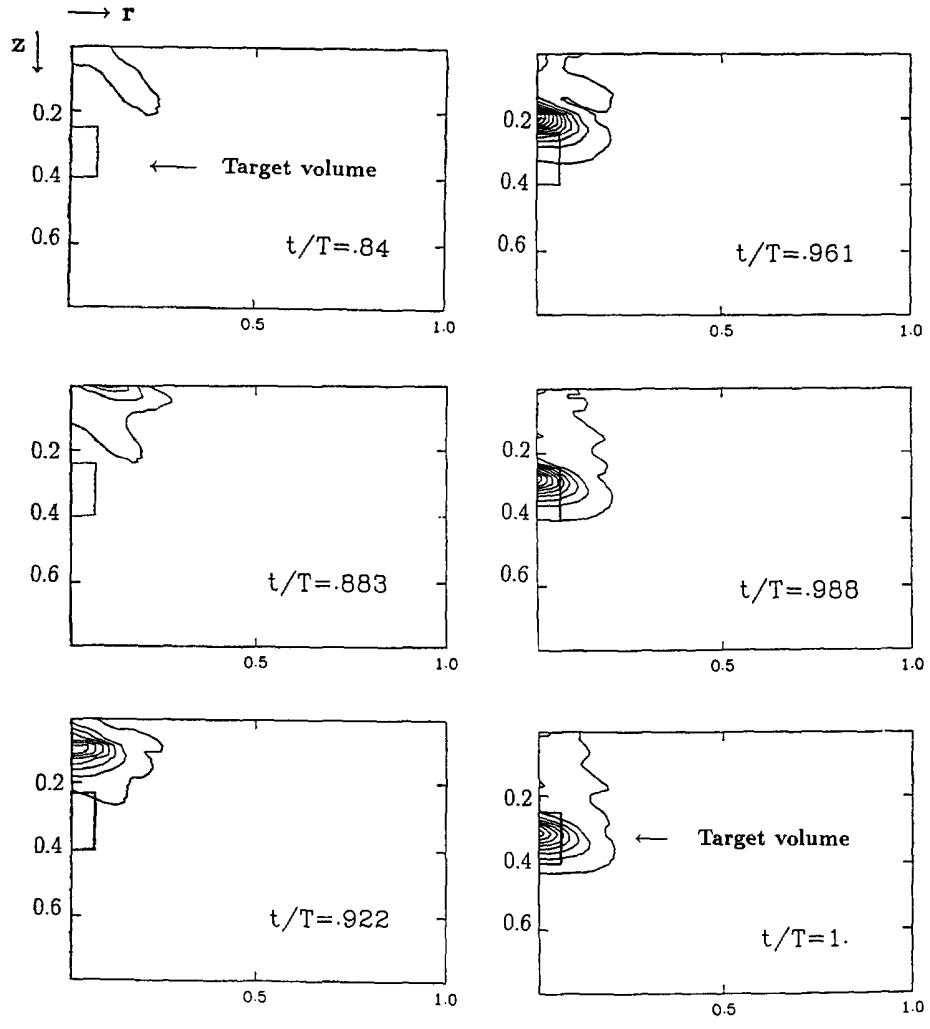

Fig. 3. Time history energy density contours in 10^{12} erg/cm^3 with the corresponding load in Fig. 2. $\varepsilon_0 = 6 \times 10^{-7}$ is the value of the energy at the first contour level, and $d\varepsilon = 2 \times 10^{-6}$ is the contour increment.

in Fig. 2, derived for a linear material model to a material with plasticity effects present, for which the constitutive equations are given above. For convergence the relaxation time η is required to be $\eta \leqslant \Delta t/5$. We use $\eta = 5. \times 10^{-9}$sec.

The propagation of the acoustic waves generated by the optimal loading was studied for increasing force amplitudes. The nominal amplitude is chosen to be the value at which yield just begins to be apparent. The loading was scaled up from the nominal amplitude by factors of 1.75 and 2.5. Figure 3 shows the time history of the energy density contours as the waves converge towards the target with the nominal loading amplitude. Comparing the amount of energy at the target to the input energy at the boundary, we note that for this case 15.5% of the energy is focused into the target. Figure 4 shows similar energy contours for the case where the loading is increased by a factor of 2.5. The amount of energy focusing into the target is 12.90% and 9.86% of the input energy for the cases of factors 1.75 and 2.5, respectively. As the loading is increased the material undergoes more plastic deformation and the amount of energy focusing at the target drops. Part of the focused target energy is spent to achieve plastic deformation. Figure 5 shows the region where plastic deformations occur at the target time ($t/T = 1$). The deformation region is centered around the target and it gets larger as the loading is increased. Figure 6 shows the time history of the strain energy at the target volume for the three loadings. For the initial loading very little residual strain is left at the target volume after the target time. For the cases where

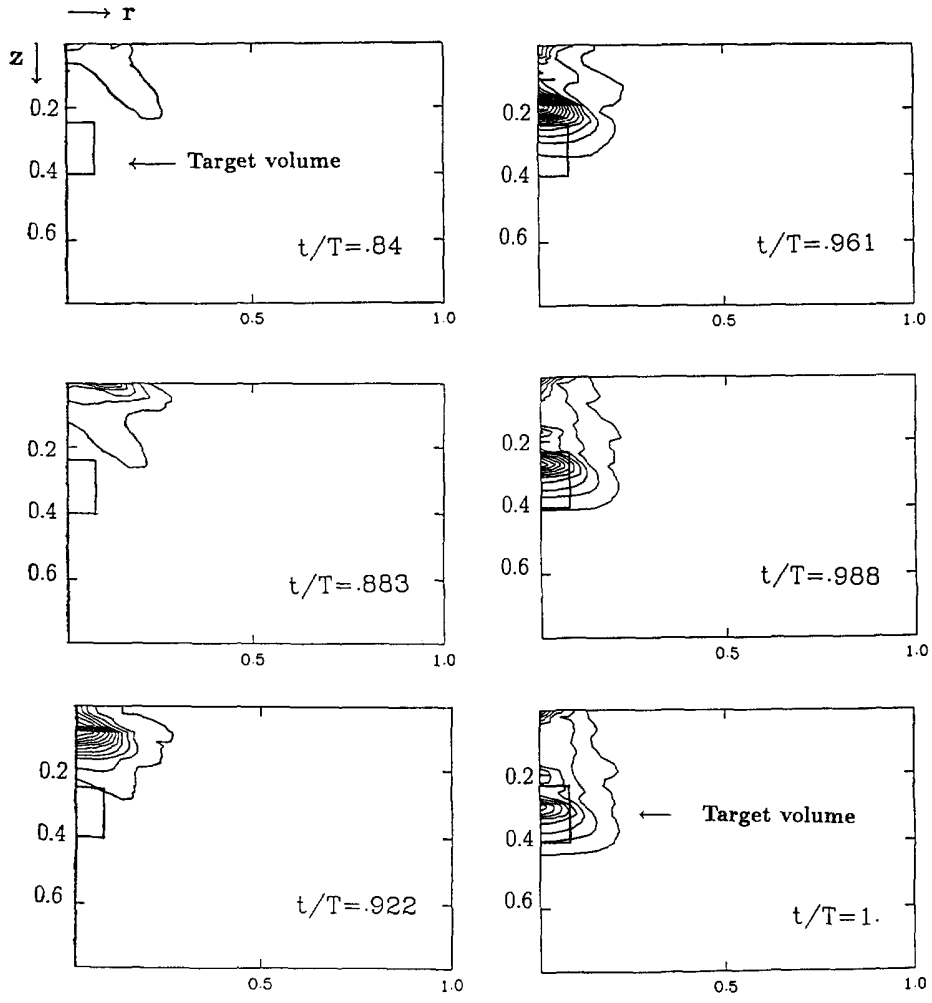

Fig. 4. Time history energy density contour in 10^{12} erg/cm^3 corresponding to the load in Fig. 2 multiplied by a factor of 2.5. $\varepsilon_0 = 3 \times 10^{-6}$, $d\varepsilon = 7 \times 10^{-6}$.

the loading is increased by factors of 1.75 and 2.5, some strain energy remains after the target time, which corresponds to a permanent signature. This is also suggested by the contour plots in Fig. 5 where for the initial loading, the process is mostly reversible except at a small region in the target volume. Figure 7 shows the time history of the second invariant of the plastic strain tensor for an element inside the target volume. The second invariant is employed here as a measure of the plastic strain tensor behavior. Figure 8 shows the time history of the kinetic energy, strain energy and the total energy in the target volume for the case where the loading is increased by a factor of 2.5. After the target time the kinetic energy tends to zero and the strain energy fluctuates around a constant value.

A summary of the results is shown in Table 1. Other cases which correspond to different choices of weight factors were also considered, but they all showed similar qualitative behavior that is presented in Table 1.

The above results also present a quantitative measure for the amplitude of the surface forces that is required in order to produce permanent deformation inside a subsurface target volume. In the cases studied here the target volume is relatively large and close to the surface. This causes the optimal loadings to have a relatively high peak amplitude at the onset of yield in the target, of about 2×10^4 N/cm^2. This compressive loading is of approximately the same magnitude as the shear yield strength. For target volumes that are located further away from the surface, the required optimal loading would be distributed over a larger surface area and would have smaller relative amplitude.

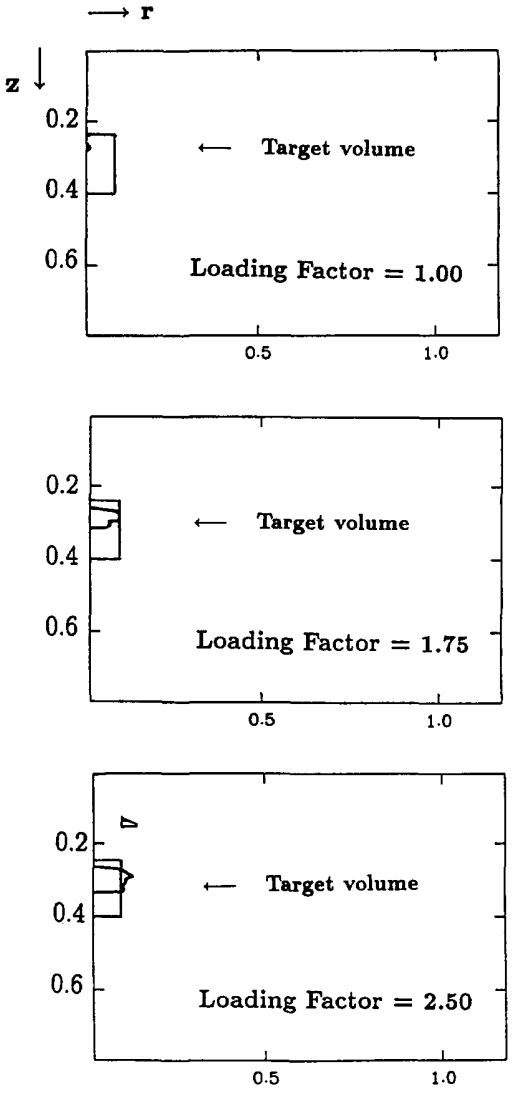

Fig. 5. Region of plastic deformation at the target time. Loading multiplied by a factor of 1.0, 1.75, 2.5.

5. CONCLUSIONS

In this paper we studied the effects of plasticity on the interior focusing of the acoustic energy. Results indicate that the optimal loadings obtained by assuming a linear elastic model for the material can produce energy focusing in a specified target volume of a visco-plastic medium. Significant plasticity effects are present around the target volume and become important as the loading is increased. It was also shown that the amount of energy

Table 1. Energy values in 10^{-4} J

Model[a]	Target energy	Input energy	% focusing
Elastic	3.237	14.00	23.10
Plastic	2.392	15.40	15.50
By 1.75	6.092	47.18	12.90
By 2.5	9.532	96.70	9.86

[a] The plastic case uses the same load as for the elastic medium. The cases by 1.75 and 2.5 refer to a plastic medium with the load increased by the indicated factor.

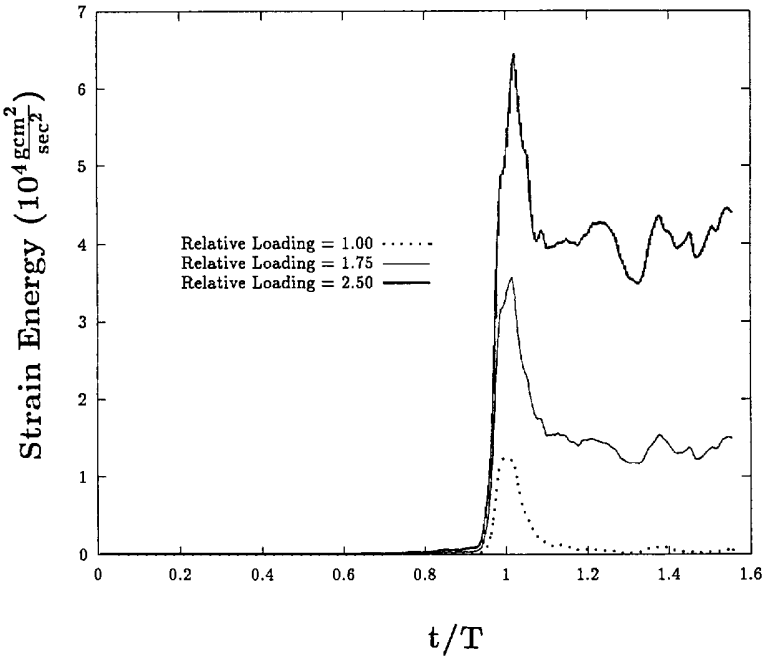

Fig. 6. Strain energy inside the target volume.

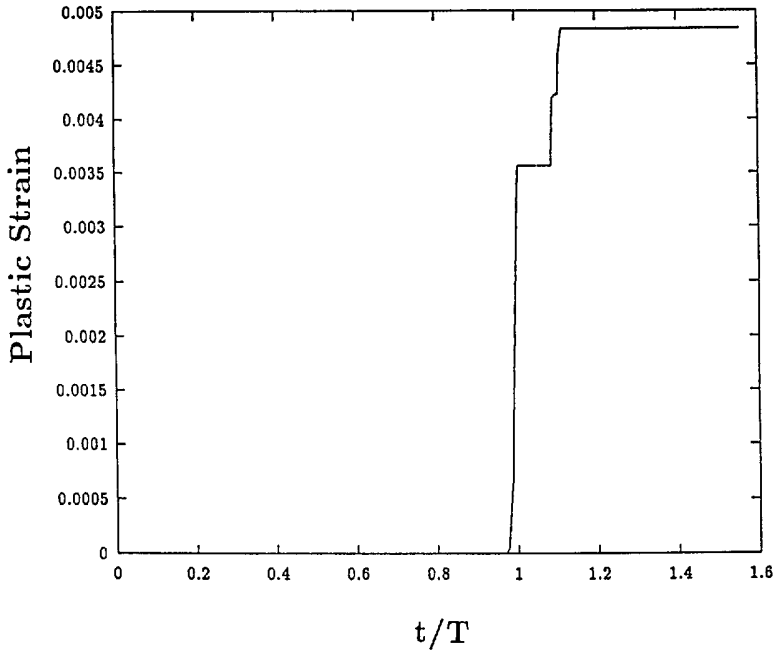

Fig. 7. Second invariant of the plastic strain tensor. Loading multiplied by a factor of 2.5.

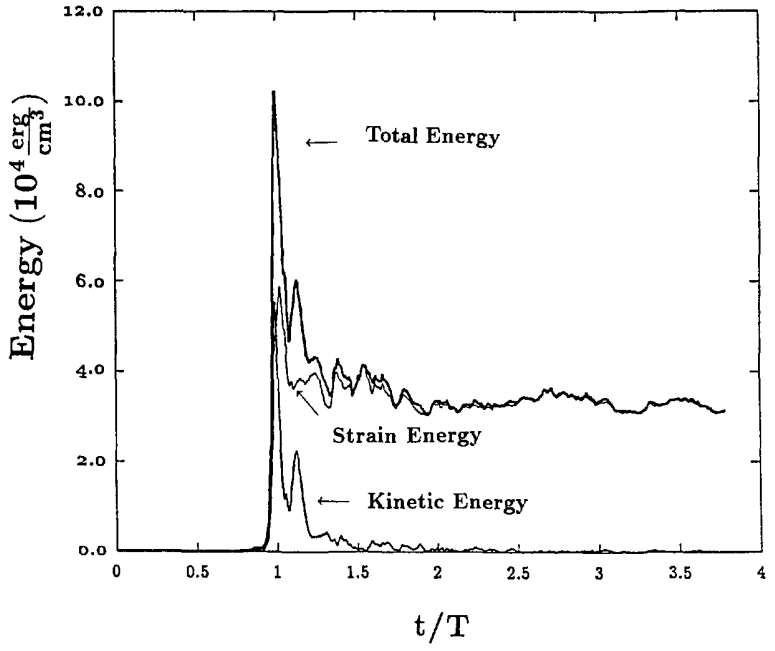

Fig. 8. Strain, kinetic and total energy inside the target volume. The loading factor is 2.5 times that of Fig. 2.

focusing with an elastic design drops as the material undergoes more plastic deformations. In all the cases the fraction of energy reaching the target is quite high. The results indicate that computationally simple optimal load designs with an elastic medium can be successfully used in a realistic elasto-plastic sample. This conclusion may have considerable significance for executing practical load designs in the laboratory.

Acknowledgements—The authors acknowledge support from the Department of Energy. Y. S. Kim acknowledges support from the Korea Science and Engineering Foundation under contract No. 951-0302-053-2, and by Hong-ik University.

REFERENCES

Boustie, M. and Cottet, F. (1991). Experimental and numerical study of laser induced spallation in aluminum and copper targets. *J. Appl. Phys.* **69,** 7533.

Cielo, P., Nodeau, F. and Lamontagne, M. (1985). Laser generation of convergent acoustic waves for materials inspection. *Ultrasonics*, March, 55–61.

Duval, G. E. and Graham, R. A. (1977). Shock induced phase transitions. *Rev. Modern Phys.* **49,** 523.

Duvaut, G. and Lions, J. L. (1972). *Les Inequations en Mecanique et en Physique*, Dunod, Paris.

Fortov, V. E., Kosin, V. V. and Eliezer, S. (1991). Spallation of metals under laser irradiation. *J. Appl. Phys.* **70,** 4524–4531.

Graff, K. (1975). *Wave Motion in Elastic Solids*. Oxford University Press, London.

Kim, Y. S., Rabitz, H., Askar, A. and McManus, J. B. (1991). Optimal control of acoustic waves in solids. *Physical Rev. B* **44,** 4892–4906.

Kim, Y. S., Tadi, M., Rabitz, H., Askar, A. and McManus, J. B. (1994). Optimal control of laser-generated acoustic waves in solids. *Physical Rev. B* **50,** 15744.

Kompfner, R. and Lemons, R. A. (1976). Nonlinear acoustic microscopy. *Appl. Phys. Lett.* **28,** 295.

Loret, B. and Prevost, J. H. (1990). Dynamic strain localization in elasto-(visco)-plastic part 1. *Computer Methods in Appl. Mech. & Engng* **83,** 247–273.

Prevost, J. H. and Loret, B. (1990) Dynamic strain localization in elasto-(visco)-plastic part 2. *Computer Methods in Appl. Mech. & Engng* **83,** 275–294.

Robinson, J. L. (1977). Fluid mechanics of copper: viscous energy dissipation in impact welding. *J. Appl. Phys.* **48,** 2202.

Scruby, C. B., Dewhurst, R. J., Hutchins, D. A. and Palmer, S. B. (1980). Quantitative studies of thermally generated elastic waves in laser-irradiated metals. *J. Appl. Phys.* **51,** 6210.

Tam, A. C. and Do, N. (1992). Laser cleaning techniques for the removal of small particles. *J. Appl. Phys.* **71,** 3515.